Investigating the impact of ferrite magnetic cores on the performance of supercapacitor assisted surge absorber (SCASA) technique

Conference Paper · June 2019

DOI: 10.1109/ISIE.2019.8781402

Sadeeshvara Udayanga Silva
University of Canterbury

Nihal Kularatna
The University of Waikato

Investigating the impact of ferrite magnetic cores on the performance of supercapacitor assisted surge absorber (SCASA) technique

Silva Thotabaddadurage Sadeeshvara Udayanga*, Nihal Kularatna† and D. Alistair Steyn-Ross‡
School of Engineering, University of Waikato, Hamilton, New Zealand
Email: *sus1@students.waikato.ac.nz, {†nihal.kularatna, ‡alistair.steyn-ross}@waikato.ac.nz

***Abstract*—Supercapacitor assisted surge absorber (SCASA) is a patented technique developed by the University of Waikato. One noticeable attribute of this design is the inclusion of a coupled-inductor which improves its capability of surge absorption.**

This paper mainly focuses on investigating the usability of ferrite iron for the core of the coupled-inductor, and attempts to explain how to minimize the effects of a negative voltage peak that arise during SCASA operation. Four ferrite cores with different geometries and material compositions (W-ferrite and J-ferrite) are subjected to 6.6 kV surge hits. Experimental outcomes demanded the need of inserting air-gaps inside these ferrite toroids. High magnetic permeability of ferrite results in a low energy storage capability; this limits their suitability in surge absorption related applications. To overcome the issues of high permeability we modified the cores with thin cuts through the surfaces. Experimental work is facilitated by lightning surge simulators (LSS-6110 and LSS-6230) coupled with the utility main to generate surge waveforms defined by the IEEE C62.41. The analysis of test results encourages us to justify the gapped-core approach, and to further verify, performance of SCASA is empirically compared for both powdered-iron cores and modified ferrite cores using international protocols of UL-1449.

***Index Terms*—SCASA, Coupled-inductor, Magnetic permeability, Powdered-iron, Ferrite-iron, LSS**

I. Introduction

Over the years, supercapacitors (SCs) have shown a promising establishment in the field of electronics with applications in many areas such as electric vehicles, renewable energy sources, UPS systems, battery-supercapacitor hybrids and cellular phones. In recent past, power electronics research group at the University of Waikato has highlighted the possibilities of using supercapacitors in novel applications [1]– [6] such as (i) efficiency enhancement in DC-DC converters (ii) surge resistant UPS designs (iii) transient surge absorption. The discovery of surge absorption capability of SCs was practically implemented in a unique design SCASA [7] that was later patented and commercialized as a practical surge protector device (SPD) by Thor technologies, Australia. This new topology carefully filters surges superimposed on utility main with the support of three main elements including a magnetic core, a SC sub-circuit and two metal oxide varistors (MOVs).

A. SCASA approach and its magnetic core

Apart from the distinction of carrying a limited number of electronic components (Fig. 1), SCASA utilizes a toroidal core that has two windings to function as a coupled-inductor. It is designed to have a lower impedance in the primary coil compared to the secondary during an event of a surge. Combined action of the two coils provide reliable protection to the active load while bulk of the surge energy is stored inside the magnetic core.

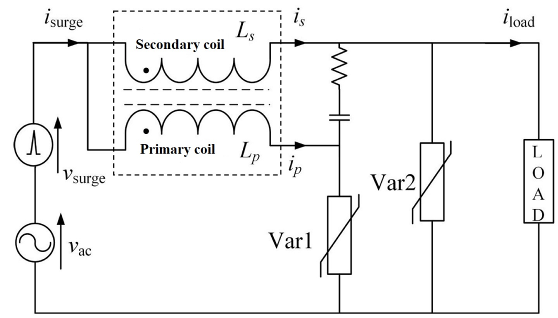

(a)

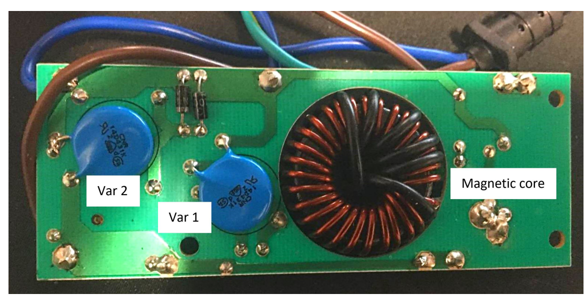

(b)

Fig. 1. SCASA design: (a) circuit diagram (b) real view of the magnetic core and associated components (MOVs: Var1 and Var2)

Original core in SCASA is made of powdered-iron, and as a prime objective of this study, the authors attempted to investigate the performance of the device using ferrite cores. Experimental approach taken is discussed in detail under the methodology. Ferrite and powdered-iron show contrasting characteristics due to the differences in their magnetic permeabilities. For example, laminated ferrite has an initial permeability of 1000-10000 H/m whereas powdered-iron lies in between 1-500 H/m [8]. This significant reduction in permeability of powdered-iron is achieved during the construction by carefully distributing air-gaps inside the material [9]. Therefore, as an alternative objective, we aimed at exploring the performance of SCASA using air-gapped ferrite cores. Another key feature of an air-gapped core is the capability of storing magnetic flux while a core composed of pure material indicates limited energy storage [10]. In section II, we present a theoretical model to examine how permeability varies with the geometry of an air column inside a gapped-core. Furthermore, we extend our model to quantify the magnetic-energy storage by an air column.

The rest of this paper is organized as follows. Section III describes the experimental set-up and methodology with a summary of properties of different toroidal cores. Then, test waveforms are discussed in detail under section IV; suitable interpretations are provided whenever required. Finally, the conclusions are drawn in section V, and a brief description about future work is also included at the end.

II. Theoretical background

A. *Effective relative permeability of an air-gapped core*

Permeability is a direct measure of any magnetic material's ability to form and sustain a magnetic field inside; hence ideal magnets show extremely high relative permeabilities. Accordingly, good magnets have very limited magnetic flux losses. In our application of SCASA, we aim to absorb part of the surge energy by eliminating part of the surge related induced flux. Coupled-inductor is the main element in this operation as eliminates surge related flux in other ways gets stored in the inductor core. Since we emphasized the importance of air-gaps, a mathematical description of its impact is presented here. For the purpose of derivations, equivalent magnetic circuits of gapped and un-gapped cores are considered.

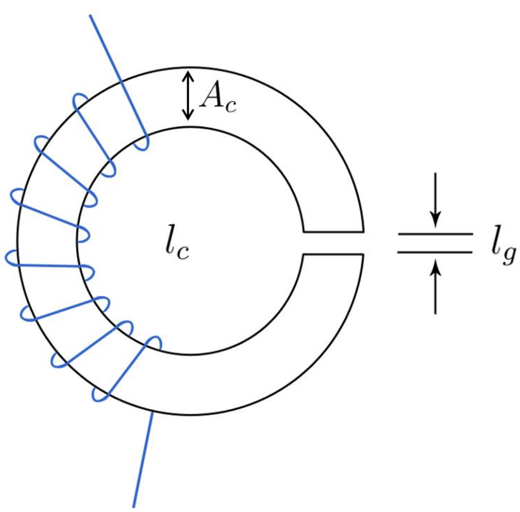

Fig. 2. Toroidal core with an air-gap

According to the definition of magnetic reluctance [11], the total reluctance $\mathcal{R}_T$ of the core with air-gap can be expressed as the sum of individual reluctances.

$$\mathcal{R}_T = \frac{l_c}{\mu_c A_c} + \frac{l_g}{\mu_\circ A_c} \tag{1}$$

Where l_c is circular length of the core, l_g is length of the air-gap, A_c is the core cross-sectional area, μ_c is the permeability of the core and $\mu_\circ$ is the permeability of free space.

By incorporating relative permeability $\mu_r = \mu_c/\mu_\circ$, we can rearrange (1) as:

$$\mathcal{R}_T = \frac{1}{\mu_\circ A_c}\left[\frac{l_c}{\mu_r} + l_g\right] \tag{2}$$

By defining an effective permeability (μ_l) considering the core as a whole, total reluctance can alternatively be written in the following form:

$$\mathcal{R}_T = \frac{l_c + l_g}{\mu_l A_c} \tag{3}$$

From (2) and (3), it is possible to obtain an expression for the effective relative permeability ($\mu_l{}'$) of the core, and this result shows how permeability of the air-gapped core varies with the gap length.

$$\mu_l{}' = \frac{\mu_l}{\mu_\circ} = l_c + l_g\left[\frac{\mu_r}{\mu_r l_g + l_c}\right] \tag{4}$$

Equation (4) is further simplified by approximating $l_c + l_g \approx l_c$ (since $l_g << l_c$); therefore, (4) reduces into:

$$\mu_l{}' = l_c\left[\frac{\mu_r}{\mu_r l_g + l_c}\right] \tag{5}$$

This result confirms the reduction of permeability in the presence of a highly reluctive (magnetically resistive) medium as air. When:

$$l_g = 0 \rightarrow \mu_l{}' = \mu_r$$
$$l_g > 0 \rightarrow \mu_l{}' < \mu_r$$

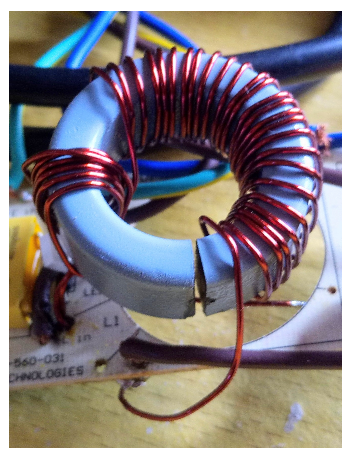

Fig. 3. Air-gapped ferrite core in SCASA

In general, it is expected that high resistive elements generate greater energy dissipations. But, in SCASA technique, air-gapped approach minimize the surge related magnetic flux by storing it rather than dissipating. So, our next aim is to develop a theoretical framework to quantify the amount of magnetic energy stored in the air-gap.

B. Magnetic energy stored in an air-gap

By applying ampere's law to the toroidal core with N number of windings:

$$\oint_L \vec{B}\cdot d\vec{l} = \sum \mu_\circ I_{en} \quad (6)$$

Where $\sum I_{en} = NI$ and $\vec{B}$ is the magnetic flux density across the core when a current I passes through the windings. Since $\vec{B}$ is uniform across any cross-section,

$$B\oint_L dl = \mu_\circ NI \quad (7)$$

Instead of considering the total circular length L, if we integrate only for the limit of air-gap l_g,

$$B = \frac{\mu_\circ NI}{l_g} \quad (8)$$

Self-inductance of a coil is defined as the magnetic flux (ϕ) per unit current $L = N\phi/I$, where $\phi = BA_c$. Using (8), we can show that the self-inductance of the air-gap $L_\circ$ is given by,

$$L_\circ = \frac{N^2\mu_\circ A_c}{l_g} \quad (9)$$

As discussed previously, the magnetic energy stored in the air-gap ($E_\circ$) helps to reduce surge energy from being transferred to the load side. Therefore, we can quantify $E_\circ$ using $\frac{1}{2}L_\circ I^2$. Using (8) and (9),

$$E_\circ = \frac{1}{2}\frac{B^2V_g}{\mu_\circ} \quad (10)$$

Here, V_g is the volume of air-body that is inserted to the toroid as indicated by Fig. 2. This air volume can be easily found using $A_c l_g$.

With the goal of verifying above discussed theoretical base, we establish our main test methods in the next section.

III. Methodology and Experimental setup

We conducted our experimental work basically in three phases. A summary of the test setup is shown in Fig. 4. Two lightning surge simulators (LSS-6110 and LSS-6230) used in our testing procedure facilitated the surge-generation as per the IEEE C62.41 standards [12].

During the initial phase, we focused on identifying the fundamental differences between ferrite and powdered-iron cores when implemented in SCASA technique. For this purpose, four ferrite cores with different geometrical configurations and different compositions (W-ferrite and J-ferrite) were installed to the SCASA circuit replacing the original powdered-iron core. But as a reference, waveforms corresponding to the original core was captured first.

Configurations of tested core types with their corresponding part numbers [13] are presented in Table I. It is noticeable that the relative permeability μ_r of W-ferrite is far greater than that of powdered-iron; therefore, to understand the significance of μ_r in detail, we considered another ferrite material (J-ferrite) which has a moderate permeability of 5000. Another key parameter of SCASA circuit is the inductance of primary and secondary coils (L_p and L_s). These two arms of the coupled-inductor carefully filter the AC mains while eliminating unwanted transient surges. Hence, in our methodology, we examined how inductances L_p and L_s vary with the insertion of different toroids. The measured values in micro-henries are tabulated in Table II.

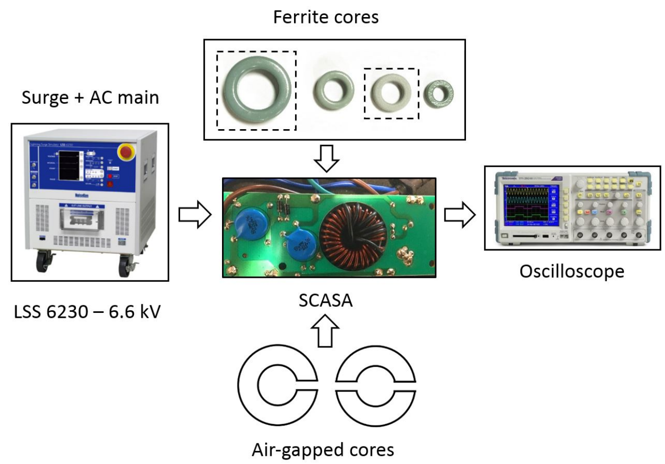

Fig. 4. Experimental setup

TABLE I
PROPERTIES OF DIFFERENT TOROIDAL CORES USED FOR TESTING

Core type and Material	Magnetics Part No.	Circular length of the Core l_c (mm)	Cross-sectional area A_c (mm^2)	Relative Permeability (μ_r)
Powdered iron (original core)	0077083A7	98.4	107	60
Ferrite (W)	ZW41605TC	37.2	15.6	10,000
Ferrite (J)	VJ42206TC	54.1	26.2	5000
Ferrite (W)	ZW42207TC	54.2	32.5	10,000
Ferrite (W)	ZW43615TC	89.6	95.9	10,000

TABLE II
INDUCTANCES OF PRIMARY AND SECONDARY COILS FOR DIFFERENT CORES TESTED

Magnetics Part No.	Relative Permeability (μ_r)	Inductance of the primary coil L_P (μH) (6 turns)	Inductance of the secondary coil L_S (μH) (28 turns)
0077083A7	60	8	120
ZW41605TC	10,000	205	4285
VJ42206TC	5000	104	2780
ZW42207TC	10,000	172	2860
ZW43615TC	10,000	340	14,740

Out of the considered ferrite cores, we detected the best possible waveforms with ZW43615TC (Fig. 6). Furthermore, it has comparably identical dimensions for both l_c and A_c with the original core. But, due to its high permeability and correspondingly high L_p and L_s, the core ZW43615TC shows limited suitability in surge absorption environment. Accordingly, as emphasized in the theory section, our next target was to continue the study by improving the surge energy absorption capability of ZW43615TC. Thus, as a satisfactory alteration we decided to incorporate air-gaps inside the core (Fig. 3).

We tested two distinct forms of air-gapped cores: one in which a thin cut of 1 mm was made through the body, and the other where the whole core body was dissected using two identical thin cuts (1 mm each). Before passing 6.6 kV surge hits to these modified cores, we measured their new inductances L_p and L_s, and the values obtained are presented in Table III. In this way, reduction of relative permeability of ferrite and the resulting changes to the inductances can be verified; hence, we can identify the most suitable air-gapped approach.

TABLE III
INDUCTANCES OF PRIMARY AND SECONDARY COILS FOR AIR-GAPPED CORES

Magnetics Part No.	No. of air gaps (l_g= 1 mm)	Inductance of the primary coil L_P (μH) (6 turns)	Inductance of the secondary coil L_S (μH) (28 turns)
ZW43615TC	0 (Ungapped)	340	14,740
ZW43615TC	1 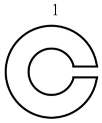	9.6	180
ZW43615TC	2 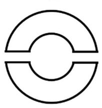	5.5	58.4

As per the measurements in Table II and Table III, we can deduce the effect of a single air-gapped core is comparable with the original powdered-iron core as in both cases L_p and L_s lie in the same range. In the case of double air-gapped core, we can identify a further reduction of inductances due to the high magnetic reluctance caused by two air columns.

During the final phase of our methodology, we aimed at investigating the performance of above modified ferrite cores in our SCASA based circuit topology. Therefore, we conducted repeated tests according to the international surge protection standards of Underwriters Laboratories (UL-1449) [14].

In the next section, we present our final test results obtained from different SCASA units composed of different cores as mentioned in Table I and Table III.

IV. TEST RESULTS AND DISCUSSION

Throughout experimentation, we used two lightning surge simulators (LSS) 6110 and 6230 for the generation of standard surge waveforms. The two most well defined waveforms [12] of 1.2/50 μs open circuit voltage waveform and 8/20 μs short circuit current waveform were coupled accurately with the utility main of 120V RMS before releasing them to the SCASA test units. Moreover, a digital oscilloscope of 100 MHz bandwidth and 1 GS/s sample rate facilitated the capturing of waveforms at the load end of SCASA devices. To interpret the operation of magnetic component under different core materials, we had capture waveforms across both the metal oxide varistors (MOV) in the SCASA circuit [15].

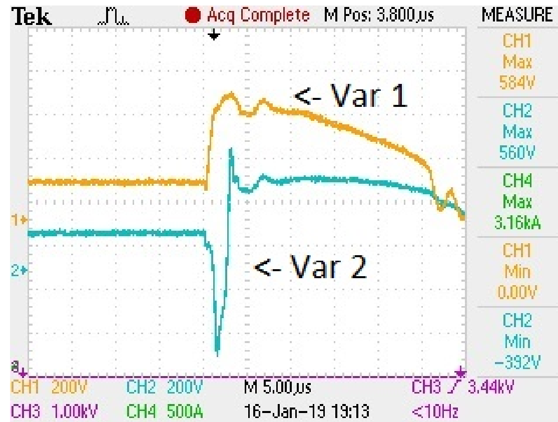

Fig. 5. Voltage variation across varistor 1 and varistor 2 after a surge hit: powdered-iron core (0077083A7)

To understand the action of coupled-inductor (magnetic component) of SCASA, we first obtained the waveforms across MOV 1 and MOV 2 with its original core (0077083A7). As indicated in Fig. 1, varistor 2 lies at the load end. The fact that varistor 2 has a reduced voltage variation compared to varistor 1 is a positive aspect of the patented SCASA technique [7]. But, as mentioned in the beginning, the negative voltage peak that arise across varistor 2 (load end) lowers the performance of this technique. To interpret this phenomenon, we must look into the induced voltages of both primary and secondary coils of the coupled inductor. These two coils are configured in such a way that the induced voltage in secondary v_s is always greater than that of the primary v_p during the propagation of a surge. Moreover, both v_s and v_p are in the same direction to oppose the incoming transient surge [16]. A clear understanding about the release of these two induced voltages can be obtained by disconnecting the supercapacitor sub-circuit of SCASA main circuit. Accordingly, Fig. 5 was captured from the oscilloscope to highlight how the difference between v_s and v_p ($v_s - v_p$) passes to the load end by causing a problematic negative voltage peak [11].

One aim of this research is to limit this negative peak; it is further understandable that an induced voltage alternatively stores magnetic energy inside a core. Therefore, our measures to reduce above explained negative peak must be very selective that it should not disturb the energy storage capability of the magnetic core.

Fig. 6 summarizes the test results for different ferrite cores indicated in Table I, and to further investigate their performance in SCASA we need to study how each core satisfies our requirements. In Fig. 6(a) to 6(c), we can observe a significant reduction in the negative peak; hence, it is tempted to think that these cores are suitable. But, the main drawback of using

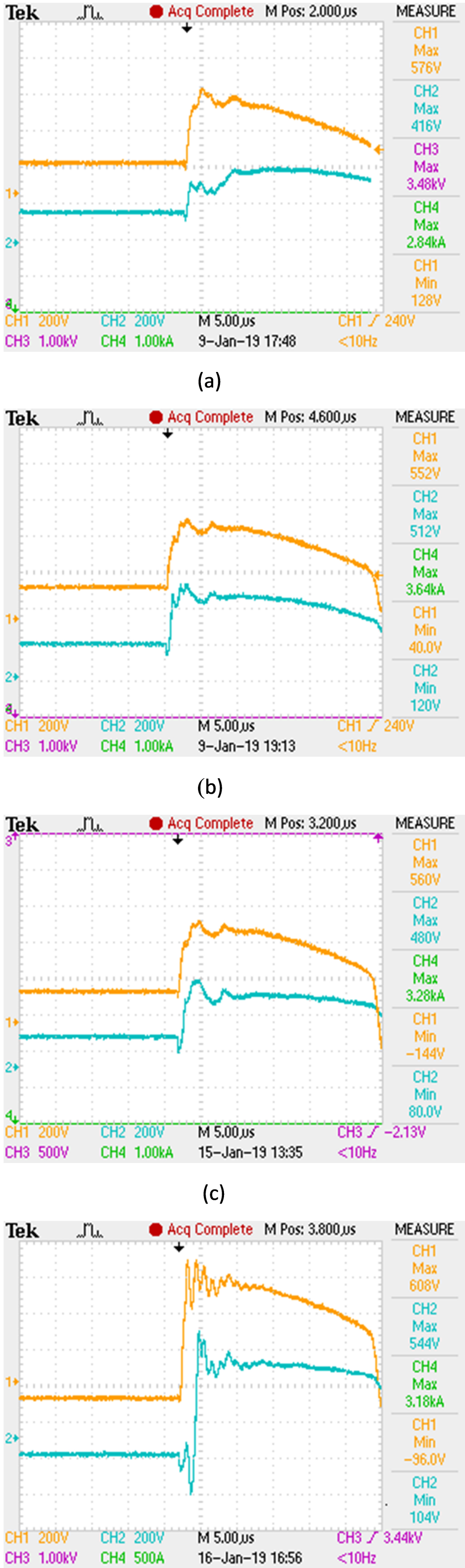

Fig. 6. Test waveforms for different ferrite cores (as in the order of Table I): (a) ZW41605TC (b) VJ42206TC (c) ZW42207TC (d) ZW43615TC

them is that they possess a very limited energy storage. As explained earlier, this reverse-sided voltage peak is another indication of how capable the core is to absorb and store surge energy in the form of induction.

Therefore, a limited surge absorption corresponds to a greater leakage of surge to the load side leading to a poorer level of protection. Accordingly, we can determine ZW43615TC which yielded Fig. 6(d) is comparably more suitable than other three cores to be installed in SCASA. Yet, its high permeability as a ferrite lowers its potential to absorb surges [17]– [18]. To overcome this problem, as suggested in the methodology, we incorporated an air column/columns (Fig. 3) to temporarily absorb and release surge energy to the environment without affecting the load side. Table III presents the two distinct forms of air-gapped approaches with associated changes to their inductances (L_p and L_s).

As a verifying step of the applicability of these modified ZW43615TC cores, we conducted consecutive surge-hit tests according to the Underwriters' Laboratory protocols (UL-1449) [14]. The outcomes are tabulated in Table IV with comparable results from the original powdered-iron core.

TABLE IV
SUMMARY OF THE PERFORMANCE OF AIR-GAPPED FERRITE CORES UNDER UL-1449 TEST PROCEDURES

Magnetics Part No.	**Original core/Modified core**	**Observations when subjected to 200 consecutive surge hits as per UL-1449**	**Effect of the negative voltage peak that passes to the load side**
0077083A7	Powdered-iron core	Survived	Observed
ZW43615TC	Ungapped ferrite core	Failed (Failure of MOV)	Partially reduced
ZW43615TC	Single gapped ferrite core	Survived	Greatly reduced
ZW43615TC	Double gapped ferrite core	Survived	Greatly reduced

V. CONCLUSION

In this paper, we mainly aimed at investigating the suitability of ferrite magnetics cores on the patented SCASA technique, and to optimize its performance using a novel approach. After studying various toroids of different compositions and geometries, we found surge absorption requirements can only be satisfied partly by the ferrite material. It was further observed that ferrites have a lesser energy storing ability compared to powdered-iron; thus, their applicability in surge absorption related areas is limited. Therefore, as a unique approach, we incorporated thin air columns to the ferrite bodies. Interestingly, this method yielded prominent test results as shown in Table IV. Alternatively, we succeeded in solving several drawbacks of the original SCASA design as well. As a verification step, we used international test procedures of

UL-1449 [14] to further examine the performance; survival under 200 consecutive surge hits (6.6 kV) substantiated the correctness of our approach. As possible future work, we plan to continue our test methods using a more powerful 15 kV surge simulator, and to enhance the surge endurance capacity of SCASA technique.

ACKNOWLEDGMENT

The authors would like to thank Ben McGuinness and Peter Higgins from the mechanical workshop at the University of Waikato for their support in drilling and cutting the ferrite materials. Their efforts provided much freedom for the authors in designing and conducting the experiments.

REFERENCES

[1] N. Kularatna, J. Fernando, K. Kankanamge, L. Tilakaratne, Very low frequency supercapacitor techniques to improve the end-to-end efficiency of DCDC converters based on commercial off the shelf LDOs, Proc. 36th Annual IECON 2010 conference of IEEE Industrial Electronics Society,2010 , pp 721 726.

[2] N. Kularatna, J. Fernando, K. Kankanamge, Xu Zhang; A Low Frequency supercapacitor circulation technique to improve the efficiency of linear regulators based on LDO chips, Proc. 26th Annual IEEE conference and exposition on Applied power electronics 2011 (APEC 11) ,2011,pp 1161 1165.

[3] N. Kularatna, J. Fernando, A supercapacitor technique efficiency improvement in linear regulators, Proc. of 35th Annual IEEE conference on Industrial Electronics, 2009, pp 132-135.

[4] N. Kularatna, and J. Fernando, High current voltage regulator United States Patent number 7,907,430, Issued March 15th 2011.

[5] N. Kularatna, L. Tilakaratne, P.K. Kumaran, Design approaches to supercapacitor based surge resistant UPS techniques 37th Annual IECON 2011 conference of IEEE Industrial Electronics Society,2011,pp 4094 - 4099

[6] U.K Madawala, D.J. Thrimawithana, N. Kularatna, An ICPT-Supercapacitor Hybrid System for Surge Free Power Transfer, in IEEE transactions on Industrial Electronics,2007,vol. 54, no.06,pp 3287 3297.

[7] J. Fernando, J.; Kularatna, N.; A supercapacitor based enhancement technique for stand-alone surge protection circuits, Proceedings of IEEE-ISIE 2013, Taipei, Taiwan, May 2013 , pp 1-7.

[8] Mag-inc.com. (2018). Magnetics - Technical Documents. [online] Available at: https://www.mag-inc.com/Design/Technical-Documents/ [Accessed 6 Jan. 2019].

[9] ”Magnetics - Powder Core Documents”, Mag-inc.com, 2018. [Online]. Available: https://www.mag-inc.com/Design/Technical-Documents/Powder-Core-Documents. [Accessed: 06- Jan- 2019].

[10] ”Air gapped magnetic cores”, Surrey.ac.uk, 2011. [Online]. Available: http://info.ee.surrey.ac.uk/Workshop/advice/coils/gap/index.html. [Accessed: 04- Jan- 2019].

[11] A. Bossche and V. Valchev, Inductors and transformers for power electronics. New York: Taylor & Francis, 2005, pp 20-54

[12] IEEE Recommended Practice on Characterization of Surges in Low-Voltage (1000 V and Less) AC Power Circuits, 2002, IEEE Standard C62.41.2

[13] ”Magnetics - Ferrite Core Documents”, Mag-inc.com, 2017. [Online]. Available: https://www.mag-inc.com/Design/Technical-Documents/Ferrite-Core-Documents. [Accessed: 10- Dec- 2018].

[14] F. Bohac, UL 1449-3rd edition effects on lightning protection systems, GE Industrial Solutions, Tech. Rep., 2010. [Online]. Available: https://apps.geindustrial.com/publibrary/checkout/UL-1449?TNR=White. [Accessed: 10- Dec- 2018].

[15] J. Fernando, N. Kularatna, H. Round and S. Tlele, ”Implementation of the supercapacitor assisted surge absorber (SCASA) technique in a practical surge protector,” IECON 2014 - 40th Annual Conference of the IEEE Industrial Electronics Society, Dallas, TX, 2014, pp. 5191-5195.

[16] J. Fernando and N. Kularatna, ”Supercapacitor assisted surge absorber (SCASA) technique: Selection of supercapacitor and magnetic components,” in Energy Conversion Congress and Exposition (ECCE). IEEE, Conference Proceedings, pp. 1992-1996.

[17] A. Bossche and V. Valchev, Inductors and transformers for power electronics. New York: Taylor & Francis, 2005, pp. 120-160.

[18] C. McLyman, Transformer and inductor design handbook. New York: Marcel Dekker, 2004, pp. 50-102.